CSCanada
Energy Science and Technology
Vol. 5, No. 1, 2013, pp. 17-25
DOI:10.3968/j.est.1923847920130501.772

ISSN 1923-8460[PRINT]
ISSN 1923-8479[ONLINE]
www.cscanada.net
www.cscanada.org

DFIG Fault Ride Through Improvement During VSC Faults

A. F. Abdou[a],*; A. Abu-Siada[b]; H. R. Pota[a]

[a] School of EIT, UNSW@ADFA, Canberra, Australia.
[b] Department of Electrical and Computer Engineering, Curtin University, Perth, WA 6845 Australia.
* Corresponding author.

Received 4 January 2013; accepted 23 February 2013

Abstract
The sensitivity of the doubly fed induction generator (DFIG) to external faults has motivated researchers to investigate the impact of various grid disturbances such as voltage sag and short circuit faults on the fault ride through (FRT) capability of the DFIG. However, no attention has been given to the impact of internal faults within voltage source converters (VSCs) that interface the DFIG with the grid, on the dynamic performance of the machine. This paper investigates the impact of various VSC faults on the dynamic performance and the FRT capability of the DFIG. Faults such as fire-through and flashover within the VSC switches are considered in this paper. Moreover, faults across the DC-link capacitor are included in this study as a common problem in the VSCs. The impact of these faults when they occur within the grid side converter (GSC) and rotor side converter (RSC) are investigated. A proper STATCOM controller to mitigate the effects of these faults on the FRT is proposed. The DFIG compliance with numerous and recently released FRT grid codes under these faults with and without the STATCOM are examined and compared. Furthermore, the capability of a proposed controller to bring the voltage profile at the point of common coupling (PCC) to the nominal steady-state level under five possible VSC faults cases is examined. The proposed controller is efficient, simple, and easy to implement.

Key words: DFIG; Fire-through; Flashover; STATCOM; FRT; VSC; RSC; GSC; Grid codes

Abdou, A. F., Abu-Siada, A., & Pota, H. R. (2013). DFIG Fault Ride Through Improvement During VSC Faults. *Energy Science and Technology*, *5*(1), 17-25. Available from: URL: http://www.cscanada.net/index.php/est/article/view/10.3968/j.est.1923847920130501.772
DOI:http://dx.doi.org/10.3968/j.est.1923847920130501.772

INTRODUCTION
Wind energy has become one of the most popular green renewable energy resources worldwide. The total global installed wind generation, during the period 1996 to 2011, was 238.351 GW (Global Wind Statistics, 2011). The use of wind energy is still growing rapidly and it is expected to provide ten percent of the global electricity generation by the year 2020 (Musgrove, 2010). Among variable speed constant-frequency wind turbines, the doubly fed induction generator (DFIG) has been popular in the wind energy conversion systems (WECS) due to its advantages (Van-Tung & Hong-Hee, 2012). DFIG has the advantage of maximum power capture, less mechanical stresses, and less acoustical noise when compared to fixed-speed induction generators (Ackermann, 2005). Compared with the full-converter variable-speed generators, the DFIG is a preferable choice in terms of size, cost, reduced losses and weight associated with the small converter (Petersson & Lundberg, 2002). The voltage source converters (VSCs) that interface with the DFIG and the ac grid are rated at 30% of the generator power capacity for a rotor speed range of ±30% (Zhe, Guerrero, & Blaabjerg, 2009). This makes the DFIG-based wind energy conversion system very sensitive to grid disturbances which may lead to catastrophic failure of the wind turbine and the converter switches if an adequate protection scheme is not installed (Lopez, Sanchis, Roboam, & Marroyo, 2007). The common solution to protect the converter from DFIG

rotor over-current is by connecting a crowbar circuit across the rotor terminals to isolate the converter from the rotor when rotor current exceeds the maximum safety margin. However, the DC-link over-voltage is controlled by a resistive chopper that can dismiss the excess energy (Rahimi & Parniani, 2010).

Statistical surveys indicate that about 38% of power converters failures are due to converter switches while 53% of their failures are attributed to faults within converters control circuits (Sethom & Ghedamsi, 2008). Another study shows that about 60% of failures within VSCs are attributed to open circuit and short circuit faults of the DC-link capacitor (Fuchs, 2003). Furthermore, a recent industry-based survey indicates that converter switches, capacitors and gate control circuits are the most susceptible components in VSC faults (Shaoyong et al., 2011).

Voltage source converters are subject to some common faults such as fire-through, flashover and DC-link faults (Arrillaga, 1998; Arrillaga, Liu, & Watson, 2007; Bin & Sharma, 2008; Bin & Sharma, 2009; K.R. Padiyar, 1990). Although most of the internal VSC transient faults are self-healed, when the cause of these faults is of a transient nature (A. F. Abdou, Abu-Siada, & Pota, 2012a, 2012b; K.R. Padiyar, 1990) they can still have a detrimental impact on the overall performance of the DFIG-based WECS (Abdou, Abu-Siada, & Pota, 2013). Researchers have given attention to the dynamic performance of DFIG-based WECS during various grid disturbances such as load fluctuation, voltage sag and swell and short circuit faults on the grid side (Campos-Gaona, Moreno-Goytia, Anaya-Lara, & Burt, 2010; He, Wang, Ma, Xu, & Han, 2009; Ibrahim, Thanh Hai, Dong-Choon, & Su-Chang, 2011; Rolan, Corcoles, & Pedra, 2011; Sheng, Xinchun, Yong, & Xudong, 2011; Xin, Tao, Yongning, & Weisheng, 2009). There are some studies about the effect of internal VSC faults on the performance of HVDC systems (Abu-Siada & Islam; Darwish, Taalab, & Rahman, 2006; Faried & El-Serafi, 1997; Xing, Tingyu, Zhen, & Renxian, 2011), but attention has not been given to investigate the impact of such faults on the overall performance of the DFIG-based WECS and its compliance to recently developed grid codes. This paper investigates the impact of various VSC faults such as fire-through flashover and DC-link capacitor short circuit faults on the fault ride through (FRT) capability of DFIGs. Under such faults, compliance of the DFIG performance with numerous FRT grid codes is also investigated.

Flexible AC transmission systems (FACTS) based power electronic converters such as static synchronous compensator (STATCOM) is being used extensively in power system applications because of its ability to provide flexible reactive power flow control (A. F. Abdou, Abu-Siada, & Pota, 2011a; K. R. Padiyar & Kulkarni, 1997). STATCOM has the ability to provide reactive power during voltage collapse with rapid response as it has no delay associated with the thyristor firing (A. F. Abdou, Abu-Siada, & Pota, 2011b; Khederzadeh, 2007). In this paper, a STATCOM controller is proposed to mitigate the effect of VSC faults on the overall performance of the DFIG-based WECS and to maintain the compliance of DFIG with various FRT grid codes during these faults.

1. SYSTEM UNDER STUDY

The single machine infinite bus (SMIB) shown in figure 1 is simulated using the EMTDC/PSCAD software to perform the investigation proposed in this paper. As shown in figure 1 the DFIG stator terminals are connected to the grid through a coupling transformer and a short transmission line while the rotor windings are fed through back-to-back IGBT-based voltage source converters with a common DC-link capacitor and chopper to limit the over-voltage of the capacitor. The grid side converter (GSC) and the RSC of the DFIG are controlled by a vector control as detailed in (Pena, Clare, & Asher, 1996; Shuhui & Haskew, 2007) and briefly elaborated below.

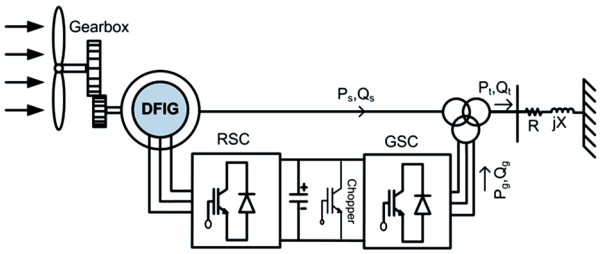

Figure 1
Single Line Diagram of the System under Study

1.1 GSC PWM Vector Control

The main task for GSC is to control the power exchange between the AC grid and the DC-link to maintain the dc voltage across the capacitor within permissible levels.

In this context, a proper reference level for the d-axis stator current i^*_{dg} is created using the voltage error signal across the DC-link capacitor. i^*_{dg} is compared with i_{dg} as shown in figure 2 to create an error signal that is used as an input to a proportional-integral (PI) controller. The level of q-axis reference current is selected to control the reactive power transfer between the GSC and the grid. The grid side controller output is used as an input to the pulse width modulation (PWM) circuit to create appropriate firing pulses for the GSC switches.

Clarke-Park transformation (Ackermann, 2005) is used to convert the stator terminal currents from the d-q reference frame to the α-β reference frame as shown in figure2 and as given below.

$$\boldsymbol{F}^{dqg}=\boldsymbol{F}^{\alpha\beta g}.e^{-j\omega_s t}=\boldsymbol{F}^{\alpha\beta g}.e^{-j\theta_s} \quad (1)$$

$$\boldsymbol{F}^{dqr}=\boldsymbol{F}^{\alpha\beta r}.e\text{-}j^{(\omega_s-\omega_r)t}=\boldsymbol{F}^{\alpha\beta r}.e^{-j(\theta_s-\theta_r)} \quad (2)$$

where $\boldsymbol{F}$ represents the voltage, current, or flux vector and the index notation g or r indicate the transformation in the grid side or the rotor side.

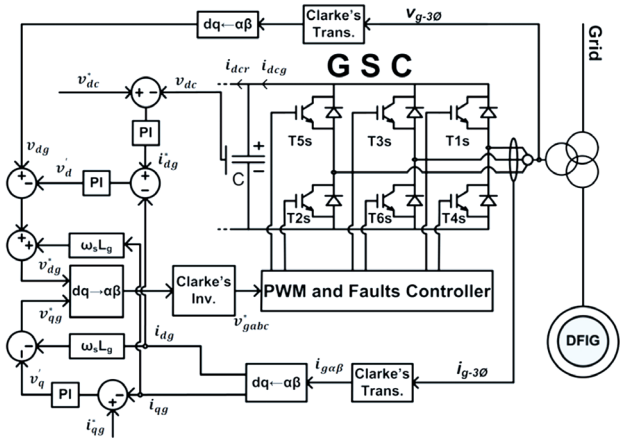

Figure 2
GSC Vector Control System

1.2 RSC PWM Vector Control

The RSC controls the generated active power according to the wind speed and the wind turbine characteristics while the reactive power command is set according to the utility requirements. As shown in figure 3, a reference signal ω^*_{pu} is selected based on the wind turbine characteristics to track the maximum power, and it is compared with the measured rotor speed to create an error signal that is fed to a PI controller to generate the q-axis rotor current i^*_{qr}. To achieve unity power factor operation, the reactive power reference Q^*_s is set to zero and is compared with the measured value to create an error signal that is fed to another PI controller to generate the reference rotor d-axis current i^*_{dr}. A Clarke-Park transformation is used to convert the d-q quantities to an a-b-c reference frame that is used as input to the RSC PWM circuit to create appropriate firing pulses for the RSC switches.

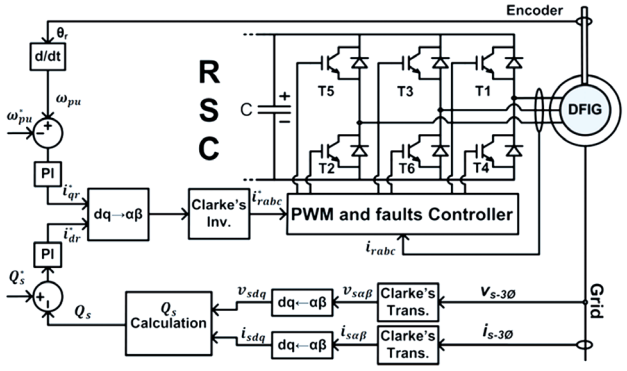

Figure 3
RSC Vector Control System

2. STATCOM MODELING

STATCOM is a shunt-connected reactive power compensation device which is capable of generating or absorbing reactive power. As shown in figure 4, STATCOM has three main components; voltage source converter (VSC) with a capacitor on the dc side, coupling transformer and the control circuit. The VSC is modeled as a six-pulse PWM GTO converter with a DC-link capacitor. The interaction between the AC system voltage and the voltage at the STATCOM AC terminals controls the reactive power flow. If the system voltage is less than the voltage at the STATCOM terminals, the STATCOM will behave as a capacitor and reactive power will be injected from the STATCOM to the system. On the other hand, if the system voltage is higher than the voltage at the STATCOM terminal, the STATCOM behaves as an inductor and the reactive power will transfer from the system to the STATCOM. Under normal operating conditions, both voltages will be equal and there will be no power exchange between the STATCOM and the AC system.

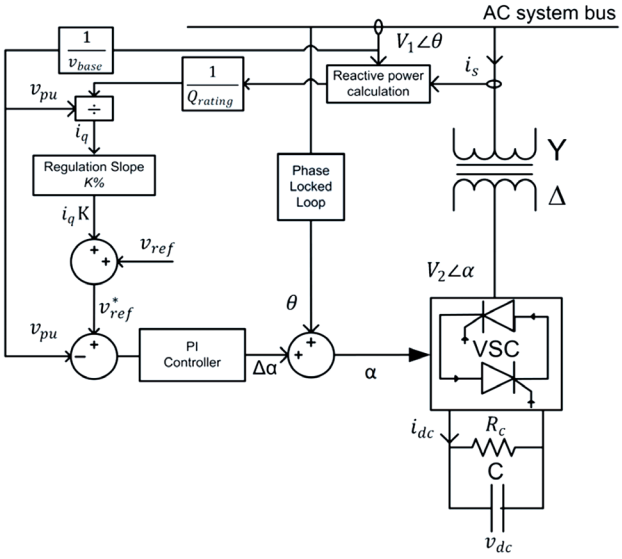

Figure 4
STATCOM Model

The reactive power exchange between the STATCOM and the AC system is controlled via controlling the VSC firing angle α to maintain the voltage at the point of connection within permissible limits. A phase-locked loop (PLL) is used to provide the phase angle θ of the point of common coupling (PCC) to assure the synchronization between the AC system and the STATCOM output voltage. Necessary filters are provided in the control scheme to limit the effects of system resonance and other harmonics (Hingorani & Gyugyi, 2000).

The linear operating range of the STATCOM can be extended if a regulation "droop" is allowed (Hingorani & Gyugyi, 2000). Regulation allows the PCC voltage to be slightly below its nominal value at full capacitive compensation and to be slightly higher than the nominal value at full inductive compensation as shown in figure 3.

A compensated signal of the compensated output current ki_q which is being negative for capacitive mode and positive for inductive mode is added to a pre-defined reference v_{ref} to create a modulating voltage reference

v^*_{ref} which is compared to the per unit voltage of the AC system to create an input to the PI controller whose output $\Delta\alpha$ is used along with θ to create the firing angle α.

The regulation slope (droop) is defined as (Hingorani & Gyugyi, 2000),

$$k = \frac{\Delta v_{Cmax}}{i_{Cmax}} = \frac{\Delta v_{Lmax}}{i_{Lmax}} \quad (3)$$

Where Δv_{Cmax} is the maximum under voltage deviation at the PCC of the STATCOM and the AC system that is corresponding to maximum capacitive output current i_{Cmax}, while Δv_{Lmax} is the maximum over-voltage deviation at the same point that is corresponding to maximum inductive output current i_{Lmax}.

The regulation slope will control the modulating voltage signal v^*_{ref} so that its value will be higher or less than the nominal reference level v_{ref} in case of inductive compensating current and capacitive compensating current respectively until the maximum capacitive or inductive compensating output current is reached as shown in figure 5.

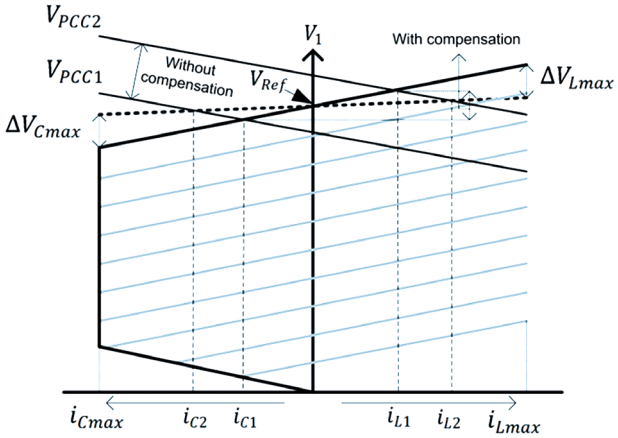

Figure 5
STATCOM V-I Characteristic

Figure 5 shows that if the voltage at the PCC is V_{PCC1}, the output compensation current is increasing from i_{C1} for a case without droop compensation to i_{C2} when droop compensation is employed. Similarly, if the voltage at the PCC increased than the nominal value (V_{PCC2}), the output compensation current will increase from i_{C1} to i_{C2}. The increase in i_C and i_L depends on the selected regulation slope as revealed in (3).

A PI controller is used to generate a proper firing angle to control the STATCOM output reactive power. The PI controller parameters are selected by using the robust optimization method Nelder and Mead (Gole, Filizadeh, & Wilson, 2005; Nelder & Mead, 1965). In this optimization method the parameters can be obtained with significantly reduced computational time and effort in comparison with traditional techniques. Nelder and Mead's algorithm adjusts the PI parameters (K_I, K_P) based on how well it minimizes the cumulative objective function (*OF*). In this paper, the objective function is represented as an integral-squared-error (*ISE*) that is widely used in steady-state and dynamic optimization problems.

$$OF = ISE = \int_{t_0}^{t_f} \left(v_{ref} + i_q k - v_{PCC}\right)^2 dt \quad (4)$$

To make the parameters selection robust, for any set of trial parameters, several system runs are conducted as shown in figure 6. An $OF(K_I, K_P)$ is determined for the entire aggregate of runs, in which each run in the aggregate corresponds to one operating condition of the network.

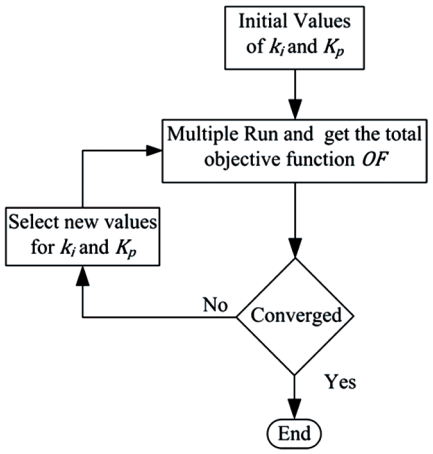

Figure 6
Flowchart for Selecting PI Parameters

3. SIMULATION RESULTS

Some VSC faults are self-clearing if the causes that lead to these faults are of a transient nature (K.R. Padiyar, 1990). However, they can still cause significant disturbances to the wind turbine and converter switches. Some faults may lead to blocking of the converter or even disconnect the wind turbine from the grid to protect them from any possible catastrophic failure. These faults can be caused by various malfunctions in the control and firing equipment (Arrillaga, 1998; Bin & Sharma, 2008).

To study the impact of various VSC faults on the voltage profile of the DFIG-based WECS, the system shown in figure 1 is used, and the crowbar protection circuit is deactivated. In all cases studied, the machine is initialized with a speed of 1.054 pu to pass the initial transients and is switched to the torque control at t= 0.5s. The STATCOM is connected to the point of common coupling of the WECS and the AC grid (bus-1 in figure 1).

In all cases studied, the voltage profile of the DFIG-based WECS with and without the STATCOM under various sustained VSC faults is examined. The faults are assumed to take place in either GSC or RSC to investigate the impact of fault location on the FRT capability of the DFIG. Time domain waveforms for the PCC reactive power, generator terminal voltage, and the voltage at

the STATCOM converter terminals (V_2 in figure 4) are investigated. Furthermore, the compliance of the voltage at the PCC of the WECS and the AC grid with various FRT grid codes such as US, Spain and Germany (Altin *et al*., 2010; Tsili & Papathanassiou, 2009) with and without the proposed controller are examined and compared.

3.1 Fire-Through

Fire-through is the conduction of a switch before its programmed instant of conduction (Arrillaga, 1998; Padiyar, 1990). A sustained fire-through of switch T3 of the RSC and GSC shown in figure 1 is assumed to take place at t = 6s. The impact of this fault on the WECS performance for each fault location is elaborated in the following section.

3.1.1 GSC Fire-Through

Figures 7-10 show the performance of the system under study during a sustained fire-through within the GSC. Figure 7 indicates that during normal operating conditions, the DFIG output reactive power is maintained at zero level to achieve the unity power factor operation as elaborated in section II. Upon fault occurrence at t = 6 s, the DFIG draws about 2.65 pu of reactive power from the grid (figure 7). The proposed controller acts to increase the voltage at the converter terminals during the fault duration as presented in figure 6. As a result, a reactive power support can be immediately provided by the STATCOM, and the reactive power at bus-1 can be regulated and maintained at zero level even though the fault is unremitting (figure 7). Figure 9 shows that the voltage at the generator terminal experiences voltage sag of 45% of its nominal value when the fault occurs at t = 6s. This voltage sag issue can be eliminated and the voltage level can be maintained at its nominal value by regulating the reactive power using STATCOM.

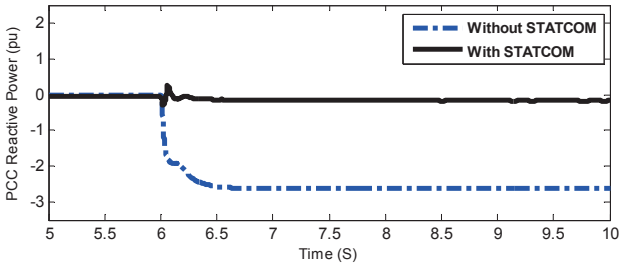

Figure 7
The PCC Reactive Power

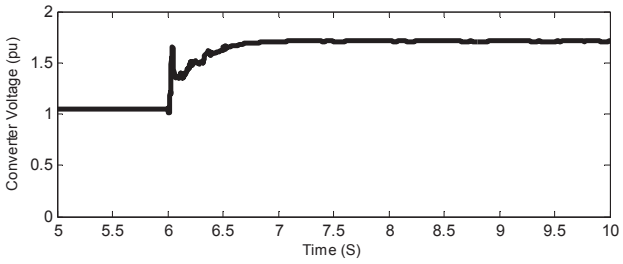

Figure 8
Converter Terminal Voltage

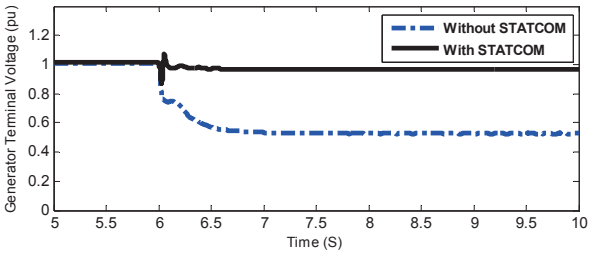

Figure 9
The Generator Terminal Voltage

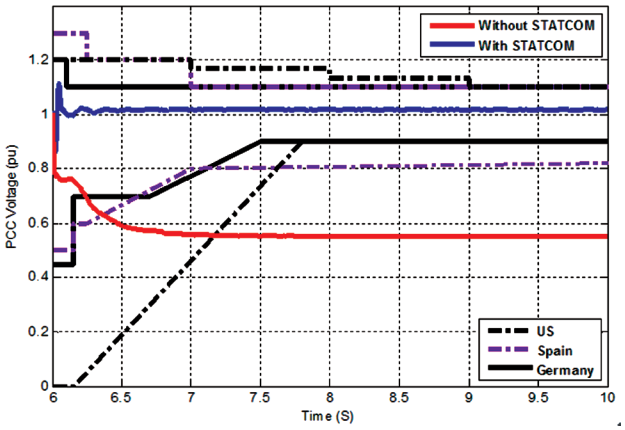

Figure 10
The PCC Voltage Compliance with the Grid Codes

Compared with FRT grid codes of the US, Spain and Germany, the voltage at the PCC will violate the low voltage ride through LVRT level of all grid codes upon the occurrence of fire-through fault at t = 6s (figure 10). This will call for the disconnection of the wind turbine from the grid. When the STATCOM is connected to the system and due to reactive power compensation, the PCC voltage is regulated to the nominal value during the fault and hence the connection of the wind turbine can be maintained.

3.1.2 RSC Fire-Through

When fire-through fault is applied to RSC, the DFIG draws about 1.8 pu of reactive power from the grid (figure 11). Figure 12 indicates that the voltage sag level at the generator terminal during the fault (25%) is less than the case of GSC fire-through. This is attributed to the fact that the GSC controller aims to maintain the voltage level across the DC-link capacitor, and hence regulating the voltage level at the PCC. Any fault within the GSC will have detrimental impact on the PCC voltage profile more than that is caused due to RSC faults. As shown in figure 13, the STATCOM controller adjusted the voltage across the converter terminal to allow the reactive power to be injected to the AC system. Without STATCOM, the voltage at the PCC violates the LVRT grid codes of the US and Germany and is on the margin of the lower level of Spain's grid code (figure12). The voltage recovery, due to the connection of the STATCOM, brings the voltage to a safety level compliant with all studied grid codes (figure 14).

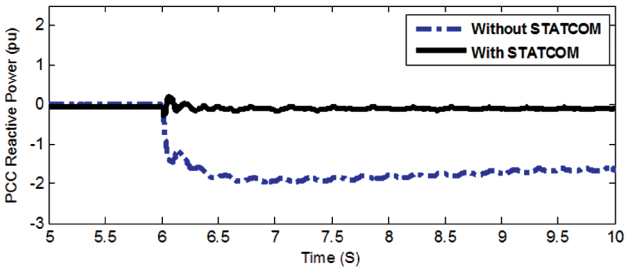

Figure 11
The PCC Reactive Power

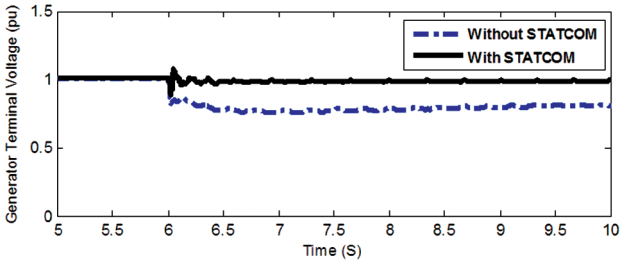

Figure 12
The Generator Terminal Voltage

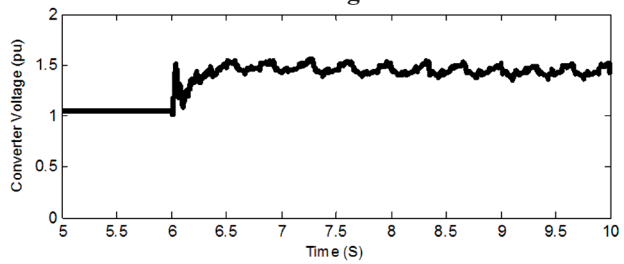

Figure 13
The Converter Terminal Voltage

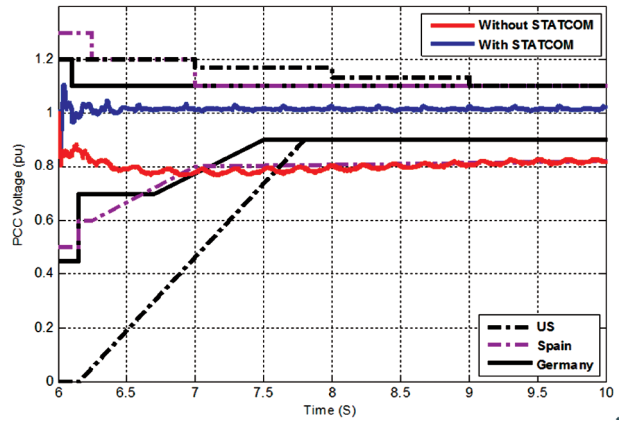

Figure 14
The PCC Voltage Compliance with the Grid Codes

3.2 Flashover

A flashover across a non-conducting switch results in a line-to line short circuit fault with a very large over-current in the conducting switch on the same side of the voltage source converter (Arrillaga, 1998; Padiyar, 1990). A flashover fault is assumed to take place at the instant that gives the maximum fault current, that is, just at the moment when a switch starts conduction.

3.2.1 GSC Flashover

A flashover is assumed to occur in switch T1 of the GSC at t = 6.21s. As a result of this fault, DFIG absorbs 2.6 pu reactive power from the grid during the fault (figure 15) and the generator terminal voltage is reduced to 0.54 pu (figure 16). The voltage at the PCC will violate the LVRT of all studied grid codes (figure 16). By connecting the STATCOM to the system, the proposed controller will adjust the converter output voltage at the instant of fault occurrence (figure 17) to provide the required reactive power support during the fault. As a result, the voltage at the PCC will be maintained within the safety margins of all studied grid codes (figure 18).

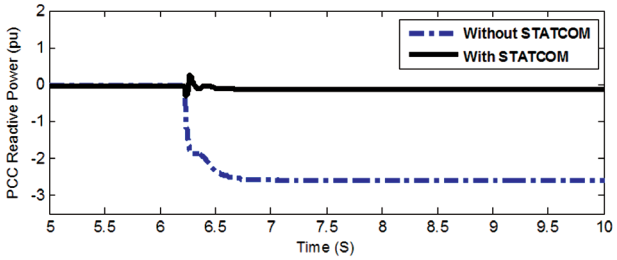

Figure 15
The PCC Reactive Power

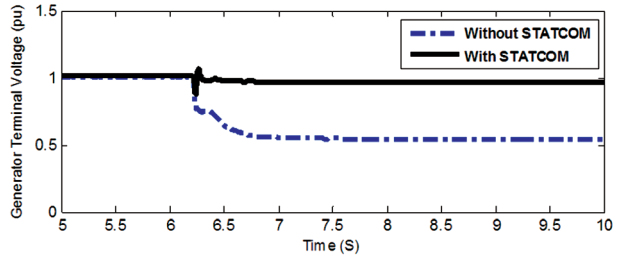

Figure 16
The Generator Terminal Voltage

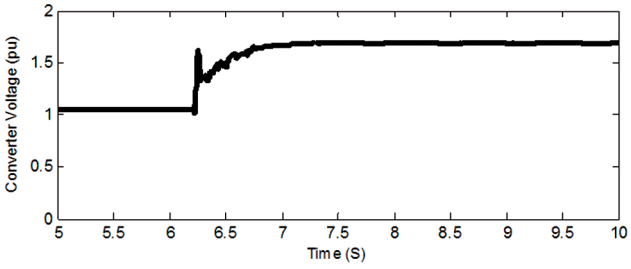

Figure 17
The Converter Terminal Voltage

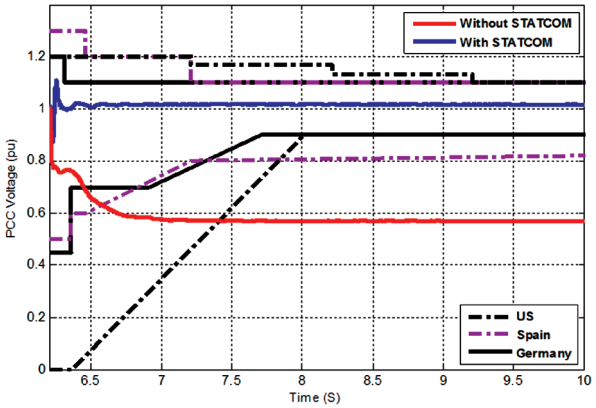

Figure 18
The PCC Voltage Compliance with the Grid Codes

3.2.2 RSC Flashover

A sustained flashover fault was simulated on switch T1 of the RSC at t = 6.31s. The impact of this fault on the DFIG voltage profile is shown in figures 17-20.

During the fault, the DFIG absorbed 1.8 pu reactive power from the grid as shown in figure 19 and the DFIG terminal voltage level was reduced to 0.75 pu (figure 20). The voltage at the PCC violated the LVRT level of the US and German grid codes, while it will be on the margin of the lower level of the FRT grid code of Spain (figure 22). The connection of STATCOM brought the reactive power and voltage at the PCC to the nominal levels as can be seen in figure 19 through 20.

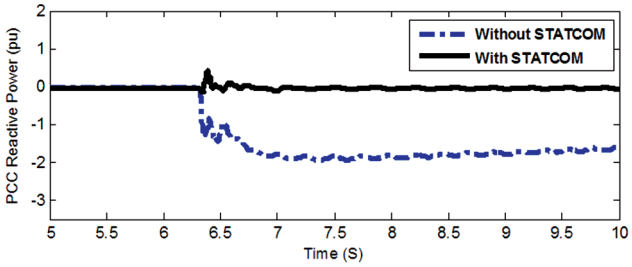

Figure 19
The PCC Reactive Power

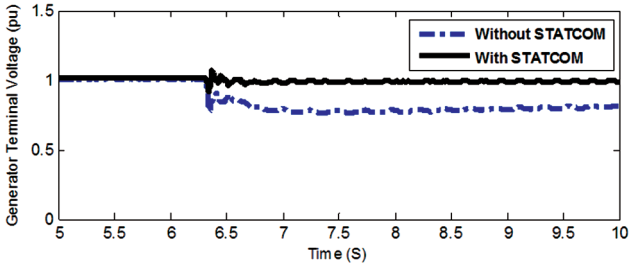

Figure 20
The Generator Terminal Voltage

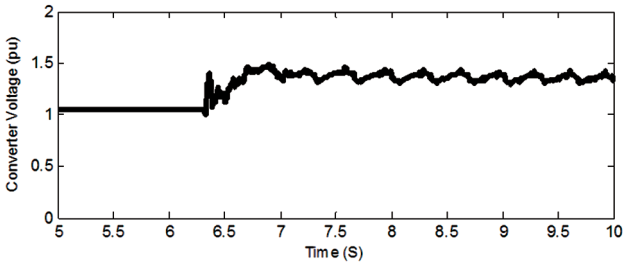

Figure 21
The Converter Terminal Voltage

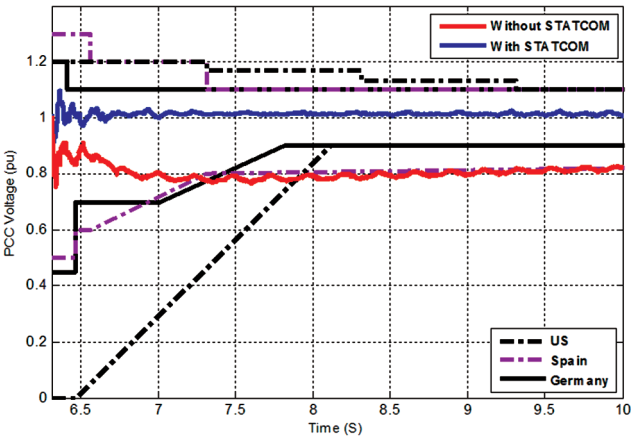

Figure 22
The PCC Voltage Compliance with the Grid Codes

3.3 Capacitor Short Circuit

The DC-link capacitor is assumed to experience a sustained short circuit fault. This type of fault is caused due to the converter high frequency applications and circuit design errors (Shaoyong *et al*., 2011). The fault is assumed to take place across the capacitor at t = 6 s. The effect of this fault on the voltage profile of the DFIG is shown in the figures 21-24.

As a result of this fault, the DFIG tended to absorb 2 pu reactive power from the grid (figure 23). The generator terminal voltage was reduced to 0.74 pu (figure 24) and the voltage at the PCC violated the LVRT level of all studied grid codes (figure 26). Again, the effect of the STATCOM controller in bringing these parameters to their normal operation levels is appreciated as revealed in figures 21-24.

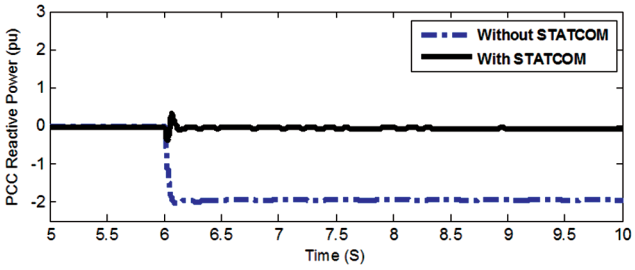

Figure 23
The PCC Reactive Power

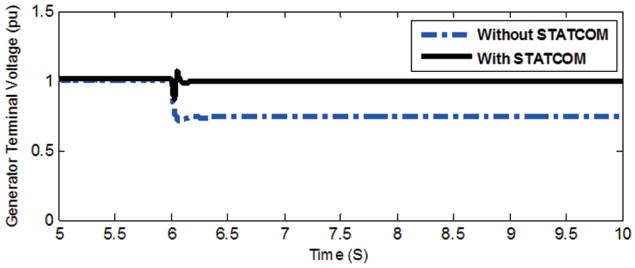

Figure 24
The Generator Terminal Voltage

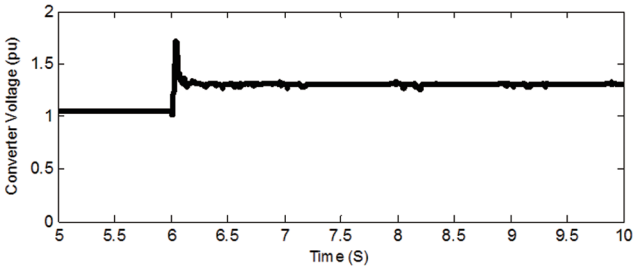

Figure 25
The Converter Terminal Voltage

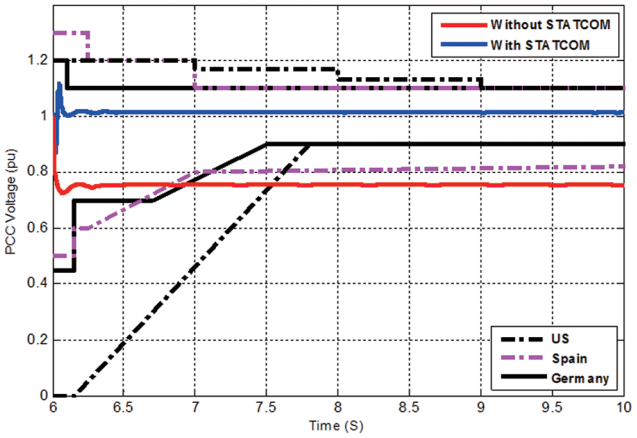

Figure 26
The PCC Voltage Compliance with the Grid Codes

CONCLUSION

In this paper, studies have been performed to investigate the impact of various DFIG voltage source converter faults on FRT capability. Simulation results show that, all studied faults namely fire-through, flashover and DC-link capacitor short circuits will lead to the violation of the LVRT levels of grid codes from the US, Germany and Spain. RSC fire-through and flashover have less impact on the voltage profile at the PCC when compared with the impact of same faults within the GSC. This is attributed to the GSC controller directly regulating the PCC voltage. Hence, any fault within the GSC will significantly affect the voltage at the PCC. If no adequate precautions are taken into account to avoid the detrimental impact of these faults on the DFIG-based WECS, the wind turbine should be disconnected from the grid to avoid any possible catastrophic failures to the turbine.

A STATCOM controller with additional droop loop and the application of a robust optimization method to adaptively tune the PI parameters is proposed to mitigate the effects of the aforementioned faults. The results demonstrate that, the proposed controller is capable of bringing the voltage profile at the PCC to the nominal steady-state level, maintaining the unity power factor operation of the DFIG and, hence, maintaining the connection of the wind turbine to the grid until either the fault is cleared or the protection scheme activated.

REFERENCES

[1] Abdou, A. F., Abu-Siada, A., & Pota, H. R. (2011a, 25-28 Sept. 2011). Application of a STATCOM for Damping Subsynchronous Oscillations and Transient Stability Improvement. Paper Presented at *the Universities Power Engineering Conference (AUPEC)*, 2011 21st Australasian.

[2] Abdou, A. F., Abu-Siada, A., & Pota, H. R. (2011b, 13-16 Nov. 2011). Damping of Subsynchronous Oscillations and Improve Transient Stability for Wind Farms. Paper Presented at *the Innovative Smart Grid Technologies Asia (ISGT)*, 2011 IEEE PES.

[3] Abdou, A. F., Abu-Siada, A., & Pota, H. R. (2012a). Application of STATCOM to Improve the LVRT of DFIG during DC-link Capacitor Failure. Paper Presented at *the Fifteenth International Middle East Power Systems Conference (MEPCON)*, 2012

[4] Abdou, A. F., Abu-Siada, A., & Pota, H. R. (2012b, 26-29 Sept. 2012). Application of STATCOM to Improve the LVRT of DFIG During RSC Fire-Through Fault. Paper Presented at *the Universities Power Engineering Conference (AUPEC)*, 2012 22nd Australasian.

[5] Abdou, A. F., Abu-Siada, A., & Pota, H. R. (2013). Effect of Intermittent Voltage Source Converter Faults on the Overall Performance of Wind Energy Conversion System. *International Journal of Sustainable Energy*, 1-13.

[6] Abu-Siada, A., & Islam, S. Application of SMES Unit in Improving the Performance of an AC/DC Power System. *Sustainable Energy, IEEE Transactions on, 2*(2), 109-121.

[7] Ackermann, T. (2005). *Wind Power in Power System*. West Sussex: John Wiley and Sons Ltd.

[8] Altin, M., Goksu, O., Teodorescu, R., Rodriguez, P., Jensen, B. B., & Helle, L. (2010, 20-22 May 2010). Overview of Recent Grid Codes for Wind Power Integration. Paper Presented at the Optimization of Electrical and Electronic Equipment (OPTIM), 2010 12th International Conference on.

[9] Arrillaga, J. (1998). *High Voltage Direct Current Transmission.* Institution of Electrical Engineers.

[10] Arrillaga, J., Liu, Y. H., & Watson, N. R. (2007). *Flexible Power Transmission: the HVDC Options*. John Wiley.

[11] Bin, L., & Sharma, S. (2008). *A Survey of IGBT Fault Diagnostic Methods for Three-Phase Power Inverters.* Paper presented at *the Condition Monitoring and Diagnosis*, 2008. CMD 2008. International Conference on.

[12] Bin, L., & Sharma, S. K. (2009). A Literature Review of IGBT Fault Diagnostic and Protection Methods for Power Inverters. *Industry Applications, IEEE Transactions on, 45*(5), 1770-1777.

[13] Campos-Gaona, D., Moreno-Goytia, E. L., Anaya-Lara, O., & Burt, G. (2010, 19-21 Oct. 2010). Ride-Through-Fault Capabilities of DFIG Wind Farm Connected to a VSC Station During a DC Fault. Paper Presented at *the AC and DC Power Transmission*, 2010. ACDC. 9th IET International Conference on.

[14] Darwish, H. A., Taalab, A. M. I., & Rahman, M. A. (2006). Performance of HVDC Converter Protection During Internal Faults. Paper Presented at *the Power Engineering Society General Meeting*, 2006. IEEE.

[15] Faried, S. O., & El-Serafi, A. M. (1997). Effect of HVDC Converter Station Faults on Turbine-Generator Shaft Torsional Torques. *Power Systems, IEEE Transactions on, 12*(2), 875-881.

[16] Fuchs, F. W. (2003, 2-6 Nov. 2003). Some Diagnosis Methods for Voltage Source Inverters in Variable Speed Drives with Induction Machines-a Survey. Paper Presented at *the Industrial Electronics Society*, 2003. IECON '03. *The 29th Annual Conference of the IEEE*.

[17] Global Wind Statistics 2011. *Global Wind Energy Council*. Retrieved from http://www.gwec.net/

[18] Gole, A. M., Filizadeh, S., & Wilson, P. L. (2005). Inclusion of Robustness into Design Using Optimization-Enabled Transient Simulation. *Power Delivery, IEEE Transactions on, 20*(3), 1991-1997.

[19] He, R.-M., Wang, J.-L., Ma, J., Xu, Y.-H., & Han, D. (2009). Impacts of DFIG-Based Wind Farm on Load Modeling. Paper Presented at *the Power & Energy Society General Meeting*, 2009. PES '09. IEEE.

[20] Hingorani, N. G., & Gyugyi, L. (2000). *Understanding FACTS: Concepts and Technology of Flexible AC Transmission Systems*. IEEE Press.

[21] Ibrahim, A. O., Thanh Hai, N., Dong-Choon, L., & Su-Chang, K. (2011). A Fault Ride-Through Technique of DFIG Wind Turbine Systems Using Dynamic Voltage Restorers. *Energy Conversion*, *IEEE Transactions on*, *26*(3), 871-882.

[22] Khederzadeh, M. (2007). *Coordination Control of Statcom and Ultc of Power Transformers*. Paper Presented at *the Universities Power Engineering Conference*, 2007. UPEC 2007. 42nd International.

[23] Lopez, J., Sanchis, P., Roboam, X., & Marroyo, L. (2007). Dynamic Behavior of the Doubly Fed Induction Generator During Three-Phase Voltage Dips. *Energy Conversion, IEEE Transactions on, 22*(3), 709-717.

[24] Musgrove, P. (2010). *Wind Power*. New York: Cambridge University Press.

[25] Nelder, J. A., & Mead, R. (1965). A Simplex Method for Function Minimization. *The Computer Journal*, *7*(4), 308-313.

[26] Padiyar, K. R. (1990). *HVDC Power Transmission Systems: Technology and System Interactions*. Wiley.

[27] Padiyar, K. R., & Kulkarni, A. M. (1997). Design of Reactive Current and Voltage Controller of Static Condenser. *International Journal of Electrical Power & Energy Systems*, *19*(6), 397-410.

[28] Pena, R., Clare, J. C., & Asher, G. M. (1996). Doubly Fed Induction Generator Using Back-To-Back PWM Converters and Its Application to Variable-Speed Wind-Energy Generation. *Electric Power Applications*, *IEE Proceedings*, *143*(3), 231-241.

[29] Petersson, A., & Lundberg, S. (2002). *Energy Efficiency Comparison of Electrical Systems for Wind Turbines*. Paper Presented at *the Nordic Workshop on Power and Industrial Electronics*, Stockholm, Sweden.

[30] Rahimi, M., & Parniani, M. (2010). Transient Performance Improvement of Wind Turbines With Doubly Fed Induction Generators Using Nonlinear Control Strategy. *Energy Conversion*, *IEEE Transactions on*, *25*(2), 514-525.

[31] Rolan, A., Corcoles, F., & Pedra, J. (2011). Doubly Fed Induction Generator Subject to Symmetrical Voltage Sags. *Energy Conversion*, *IEEE Transactions on*, *26*(4), 1219-1229.

[32] Sethom, H. B. A., & Ghedamsi, M. A. (2008). Intermittent Misfiring Default Detection and Localisation on a PWM Inverter Using Wavelet Decomposition. *Journal of Electrical Systems, 4*(2). 222-234.

[33] Shaoyong, Y., Bryant, A., Mawby, P., Dawei, X., Li, R., & Tavner, P. (2011). An Industry-Based Survey of Reliability in Power Electronic Converters. *Industry Applications*, *IEEE Transactions on*, *47*(3), 1441-1451.

[34] Sheng, H., Xinchun, L., Yong, K., & Xudong, Z. (2011). An Improved Low-Voltage Ride-Through Control Strategy of Doubly Fed Induction Generator During Grid Faults. *Power Electronics*, *IEEE Transactions on*, *26*(12), 3653-3665.

[35] Shuhui, L., & Haskew, T. A. (2007). *Analysis of Decoupled d-q Vector Control in DFIG Back-to-Back PWM Converter*. Paper Presented at *the Power Engineering Society General Meeting*, 2007.

[36] Tsili, M., & Papathanassiou, S. (2009). A Review of Grid Code Technical Requirements for Wind Farms. *Renewable Power Generation*, *IET*, *3*(3), 308-332.

[37] Van-Tung, P., & Hong-Hee, L. (2012). Performance Enhancement of Stand-Alone DFIG Systems With Control of Rotor and Load Side Converters Using Resonant Controllers. *Industry Applications, IEEE Transactions on, 48*(1), 199-210.

[38] Xin, L., Tao, Z., Yongning, C., & Weisheng, W. (2009, 27-31 March 2009). Short Circuit Current Characteristic of Wind Generators. Paper Presented at *the Power and Energy Engineering Conference*, 2009. APPEEC 2009. Asia-Pacific.

[39] Xing, Z., Tingyu, Q., Zhen, X., & Renxian, C. (2011, 15-17 July 2011). Dynamic Analysis of Doubly Fed Induction Generator During Symmetrical Voltage Swells. Paper Presented at *the Mechanic Automation and Control Engineering (MACE)*, 2011 Second International Conference on.

[40] Zhe, C., Guerrero, J. M., & Blaabjerg, F. (2009). A Review of the State of the Art of Power Electronics for Wind Turbines. *Power Electronics, IEEE Transactions on, 24*(8), 1859-1875.

